Pollutants, pathogens and public transport - ventilation, dispersion and dose

Chris Baker

November 2021

1. Introduction

The ventilation of buses and trains has come to be of some significance to the travelling public in recent years for a number of reasons. On the one hand, such vehicles can travel through highly polluted environments, such as urban highways or railway tunnels, with high levels of the oxides of nitrogen, carbon monoxide, hydrocarbons and particulate matter that can be drawn into the passenger compartments with potentially both short- and long-term health effects on passengers. On the other, the covid-19 pandemic has raised very significant concerns about the aerosol spread of pathogens within the enclosed spaces of trains and buses. There is a basic dichotomy here - to minimise the intake of external pollutants into vehicles, the intake of external air needs to be kept low, whilst to keep pathogen risk low, then high levels of air exchange between the outside environment and the internal space are desirable. This paper addresses this issue by developing a common analytical framework for pollutant and pathogen dispersion in public transport vehicles, and then utilises this framework to investigate specific scenarios, with a range of different ventilation strategies.

In the next section, we present some of the relevant background literature and identify the major pollutant pathways. Section 3 sets out a basic analytical model, that considers both externally and internally generated pollutants and pathogens to be considered in a common ventilation framework, whist making no assumptions about the ventilation mechanisms. This of itself offers some useful insights into the differences between externally and internally generated pollutants. Section 4 then considers the nature of the ventilation of public transport vehicles and identifies the important parameters that govern ventilation rate. The basic model is utilised to study a number of specific scenarios in section 5. Some broad conclusions are drawn in section 6.

2. Background

Since the 1980s many investigations have been carried out of pollutant levels in traffic environment - see for example the work of Hicks et al (2021) at a heavily congested roadside site in London, and that of Hickman et al (2018) and Font et al (2020) for enclosed railway stations. More recently, a number of investigators have measured pollutant levels within the passenger compartments of trains and buses, in a variety of different environments. These include metro and commuter rail systems in Czechia (Branis, 2006), South Korea (Park et al, 2008), Taiwan (Cheng et al, 2012), Greece (Maggos et al, 2016), Canada (Heong et al, 2017), Sweden (Cha et al, 2018a,b), Denmark (Anderson et al 2019a,b), the Philippines (Batutay et al, 2020) and Portugal (Buitrago et al, 2021), with measurements made on both underground and overground trains. Measurements made on urban buses are reported from China by Li et al (2017) and from India by Chaudhry and Elumalai (2020).

From these investigations the following major points emerge.

- The main concern is with pollutants that arise from diesel engines, whether in trains or buses. These include the oxides of nitrogen, carbon monoxide, a range of hydrocarbons and particulate matter over a large size range, all of which can cause respiratory problems at elevated concentrations or can be toxic at higher concentrations.
- Diesel trains have much higher levels of all pollutants than electric trains.
- Particulate matter can also be the result of brake wear or road or rail wear.
- For diesel trains, the roof mounted engine exhausts can be in close proximity to the inlets to HVAC systems, with regular plume impingement and thus pollutant can be ingested into the passenger cabin.
- Pollutant levels varied significantly with position within trains, the train consist and whether or not the locomotive was leading or trailing.
- For road vehicles in congested urban areas, the pollutants of concern can arise from all the traffic on the road, dispersed by the vehicle wakes, forming a cloud of pollutant over the highway that can again be ingested into the air conditioning systems or through open windows.
- Similarly in enclosed railway stations, concentrations of diesel pollutants can be significantly above ambient levels.
- Less directly, particulate matter from vehicles and other sources, can be deposited in road or rail environments, particularly enclosed tunnels, resuspended by vehicle movement and then ingested into passenger compartments. In such cases interior concentration of pollutants can be very high.

Pollutants can also be generated internally within vehicles. Carbon dioxide from passenger respiration, which, if allowed to build up, can cause drowsiness and headaches, or more severe symptoms. In addition, pathogens, such as flu or covid-19, can be generated within passenger compartments by infected individuals and have the potential to infect others. This latter aspect has not been extensively studied, although there is some recent CFD based work reported in Zhang et al, (2012), Wang et al (2014) and Peng et al (2020). It is now generally recognised that pathogen transmission is primarily by aerosols, with transmission by larger droplets only occurring between individuals in close proximity - see the recent review by Wang et al (2021), which shows that the evidence for transmission by surface contamination is surprisingly weak.

Finally, there is an emerging body of evidence that high levels of pollutant can increase the risk of pathogen infection. Long term exposure to particulate pollutants in particular can results in a weakened respiratory system that makes individuals more prone to infection and serious illness (Mein et al, 2020; Comunian et al, 2020, Travaglio et al, 2021). There are also indications (although not strong) that particulates in the atmosphere can act as foci for pathogens that increase the local risk of transmission (Nor et al, 2021).

3. Analysis

3.1 Formulation of concentration equation

In the analysis that follows, we consider the build-up of both pollutants or pathogens in a public transport vehicle using a unified approach based on simple conservation arguments. This approach is not novel and has been used by others (eg Miller et al, 2021), but here we aim to treat the issues in a unified way within a common framework. We assume that the vehicle is ventilated either naturally through openings, or through a number of HVAC systems. There may or may not be the facility for air recirculation and cleaning. The equation of conservation of pollutant or pathogen mass is given in words as follows

Rate of change of mass of species inside the vehicle = inlet mass flow rate of species + mass generation rate of species within the vehicle - outlet mass flow rate of species– mass flow rate of species removed through cleaning, deposition on surfaces or decay.

"Mass" here is defined differently for pollutants and pathogens - in the standard way as kilograms for chemical pollutants, and as quanta for pathogens. Concentrations are similarly defined in two ways - as kilograms of pollutant per kilogram of air, or as quanta of pollutant per kilogram of air.

In symbols this conservation equation can be written

$$\rho V \frac{dC}{dt} = \sum \dot{m}_i C_i + g - C \sum \dot{m}_i - \dot{m}_c C\epsilon - \rho V C\gamma - \rho V C\delta \quad (1)$$

Here ρ is the density of air (kg/m^3); V is the internal volume of the vehicle (m^3); C is the internal concentration in the vehicle (kg/kg or quanta/kg); t is time (h); $\dot{m}_i$ is the mass flow rate of air at ventilation inlet *i* (kg/h); C_i is the concentration of species at inlet *i* (kg/kg or quanta/kg); g is the internal generation term in (kg/h or quanta/h); $\dot{m}_c$ is the recirculated mass flow of air (kg/h); ϵ is the cleaning efficiency of the recirculation system; γ is the rate of deposition to surfaces (1/h) and δ is the decay rate of the pollutant or pathogen (1/h) .

The mass flow rates will depend upon the type of opening and for non-airconditioned vehicles will be a function of vehicle speed. At this stage we make no specific assumptions about the nature of the ventilation system, other than it draws in air through a number of inlets and may or may not offer the facility for recirculating and cleaning a portion of that air.

We now define equivalent mass flow rates and concentrations.

$$\dot{m}_e = \sum \dot{m}_i \quad (2)$$

$$C_e = \frac{\sum \dot{m}_i C_i}{\sum \dot{m}_i} \quad (3)$$

The conservation equation becomes

$$\rho V \frac{dC}{dt} = \dot{m}_e C_\mathrm{e} + g - \dot{m}_e C - \dot{m}_c C\epsilon - \rho V C\gamma - \rho V C\delta$$

After some manipulation this becomes

$$\frac{dC}{dt} = \alpha C_\mathrm{e} + \frac{g}{\rho V} - (\alpha + \beta + \gamma + \delta)C$$

where α is the number of air changes through the vehicle ventilation system per hour and is given by

$$\alpha = \frac{\dot{m}_e}{\rho V} \quad (4)$$

and β is the rate of recirculation of clean air per hour given by

$$\beta = \frac{\dot{m}_c \epsilon}{\rho V} \tag{5}$$

3.2 Solutions of concentration equations

This equation is very straightforward and applies to both pollutants and pathogens, provided the terms are appropriately defined. We now consider two cases - the concentrations from external sources (for example, external sources of the oxides of nitrogen or particulate matter); and the concentrations due to internal pollutant or pathogen generation (for example, carbon dioxide or Covid-19).

For external pollutants, the internal generation term is zero. The concentration equation then becomes

$$\frac{dC}{dt} = aC_{\mathrm{e}} - (\alpha + \beta + \gamma + \delta)C \tag{6}$$

This can be straightforwardly solved for internal concentrations for arbitrary time histories of external concentration and also various air recirculation strategies (such as turning HVAC systems on and off, or closing and opening windows). If C_{e}, a, β, γ and δ are constant and the initial concentration is zero, we have the very simple solution

$$C = \frac{\alpha C_e}{(\alpha+\beta+\gamma+\delta)}\left(1 - e^{-T(\alpha+\beta+\gamma+\delta)}\right) \tag{7}$$

where T is the journey time. For large values of T this becomes

$$C_\infty = \frac{\alpha C_e}{(\alpha+\beta+\gamma+\delta+\delta)} \tag{8}$$

and one can thus write

$$C = C_\infty\left(1 - e^{-T(\alpha+\beta+\gamma+\delta)}\right) \tag{9}$$

For internal pollutants, we assume that the internal source is the passenger load, and we write

$$g = Nq_o \tag{10}$$

where N is the total number of passengers when pollutants such as carbon dioxide are being considered, or the number of infected passengers when pathogens are being considered. q_o is the output of pollution per person in kg/h or of pathogen in quanta/h. The conservation equation becomes

$$\frac{dC}{dt} = \frac{Nq_o}{\rho V} - (\alpha + \beta + \gamma + \delta)C \tag{11}$$

Here concentrations are expressed as kg of pollutant / kg of air or quanta of pathogen / kg of air. Again, this can be readily solved numerically for variable values of C_{e}, q_o, a etc. As in the external pollutant case, it has a simple solution for C_{e}, q_o, a, ϵ and r are constant and an initial concentration of zero.,

$$C = \frac{Nq_o}{\rho V(\alpha+\beta+\gamma+\delta)}\left(1 - e^{-T(\alpha+\beta+\gamma+\delta)}\right) \tag{12}$$

with the solution for large time as

$$C_\infty = \frac{Nq_o}{\rho V(\alpha+\beta+\gamma+\delta)} \tag{13}$$

and again

$$C = C_\infty\left(1 - e^{-T(\alpha+\beta+\gamma+\delta)}\right) \quad (14)$$

Now let us consider the implications of the above equations. For externally or internally produced gaseous pollutants the sum $(\alpha + \beta + \gamma + \delta)$ that appears in the above analysis simplifies to $(\alpha + \beta)$ since there is no deposition and no pollutant decay. For particulate pollutants this term becomes $(\alpha + \beta + \gamma)$ whilst for pathogens all the terms are important. If there is no air recirculation with $\beta = 0$, then for gaseous pollutants the sum simply becomes equal to α and for particulates to $\alpha + \gamma$

At this point it is worth considering the relative magnitudes of α, β, γ and δ. It will be shown in the next section that α for most ventilation mechanisms is of the order of 10/h. Jimenez and Peng gives values of β, γ and δ for a range of ventilation systems of around 3, 0.2 and 1.6. The value for γ is quite general and applies to PM2.5 to PM10 particles and also for pathogens, whilst the value for δ is specifically for covid-19. Thus for both gaseous and particulate pollutants with no recirculation the sum $(\alpha + \beta + \gamma + \delta)$ is dominated by α. Now equations (7) to (9) therefore suggest that the internal concentrations of pollutants that are generated outside the vehicle, in the absence of recirculation of air within the vehicle, deposition or decay, tend in the long term to the weighted average of the concentrations at the inlets, be they HVAC systems or windows and doors. These long-term values are (2021) independent of air exchange rates. The air exchange rates do however affect the rate at which the concentrations approach the long-term values. In contrast for internally generated pollutants of pathogens, equations (12) to (14) suggest the long-term values are very dependent upon air exchange rates even when there is no recirculation, decay or deposition, and low rates of air exchange can lead to high internal concentrations. Again, the air exchange rates affect the speed with which the long-term values are reached. For both external pollutants and internally generated pollutants, the concentrations can be significantly reduced by recirculation and cleaning of the air.

In the above equations $T = 1/(\alpha + \beta + \gamma + \delta)$ is effectively the time for one air change. Equations (9) and (14) indicate that after one air change the concentration is 63% of its long-term value, and this rises to 98% after 4 air changes.

3.3 Dose calculations

The dose of pollutant or pathogen received can then be calculated from

$$d = q_i T \bar{C} \quad (15)$$

where q_i is the rate of breathing in, T is the journey time and $\bar{C}$ is the average concentration over the course of the journey.

For external pollutants the average concentration for a journey where the initial concentration is zero

$$\bar{C} = \frac{\alpha C_e}{(\alpha+\beta+\gamma+\delta)}\left(1 - \frac{\left(1-e^{-T(\alpha+\beta+\gamma+\delta)}\right)}{T(\alpha+\beta+\gamma+\delta)}\right) \quad (16)$$

which gives a dose of

$$d = \frac{q_i T \alpha C_e}{(\alpha+\beta+\gamma+\delta)}\left(1 - \frac{\left(1-e^{-T(\alpha+\beta+\gamma+\delta)}\right)}{T(\alpha+\beta+\gamma+\delta)}\right) \quad (17)$$

and a dose for a long journey of

$$d_\infty = \frac{q_i T \alpha C_e}{(\alpha+\beta+\gamma+\delta)} \quad (18)$$

For Internal pollutant or pathogen generation the average concentration is

$$\bar{C} = \frac{Nq_o}{\rho V(\alpha+\beta+\gamma+\delta)} \left(1 - \frac{\left(1-e^{-T(\alpha+\beta+\gamma+\delta)}\right)}{T(\alpha+\beta+\gamma+\delta)}\right) \quad (19)$$

and the dose becomes

$$d = \frac{q_i T N q_o}{V(\alpha+\beta+\gamma+\delta)}\left(1 - \frac{\left(1-e^{-T(\alpha+\beta+\gamma+\delta)}\right)}{T(\alpha+\beta+\gamma+\delta)}\right) \quad (20)$$

with the asymptotic dose given by

$$d_\infty = \frac{q_i T N q_o}{V(\alpha+\beta+\gamma+\delta)} \quad (21)$$

In health terms the dose of pollutant or pathogen is an important parameter. This is not well specified, with standards for pollutants usually taking the form as the average concentration allowed over a certain period (usually one or twenty-four hours). For example, the EU limits for Nitrogen Dioxide are 200 μg/m^3 over a one-hour period, which must not be exceeded more than 18 times in any one year (EU, 2021). Similarly, the limit for PM10 is 50 μg/m^3 over a twenty-four-hour period. Carbon Dioxide by contrast simply has a maximum concentration level specified in CDC (2021) of 5000 ppm. By contrast pathogen dose is utilised in the determination of infection probabilities, and it is that issue to which we now turn.

3.4 Infection probabilities

We now consider in more detail the infection probability due to pathogen dose. We follow the methodology of Jimenez and Peng (2021) but adopt a simplified analytical form that throws considerable light on the problems. Note that what follows implicitly assumes complete mixing of the pathogen across the passenger compartment, which is clearly an idealisation, and does not take into account the greatly elevated concentrations around infected individuals. We discuss how this might be allowed for in the future below.

The probability of infection with the pathogen P is given by

$$P = \left(1 - \left(1 - p\left(1 - e^{-d}\right)\right)^{N-1}\right) K\,(1 - f_I)(1 - f_m\epsilon_i)(1 - f_m\epsilon_o) \quad (22)$$

Here p is the population probability of infection; K is a factor that allows for pathogen variants; f_I is the fraction of people who are immune due to vaccination or previous infection; f_m is the fraction of people wearing masks; ϵ_o is the mask efficiency for breathing out; and ϵ_i is the mask efficiency for breathing in. For small values of d and p this can be approximated by

$$P = dp(N-1)K\,(1 - f_I)(1 - f_m\epsilon_i)(1 - f_m\epsilon_o) \quad (23)$$

For the general case equations (15) and (26) give

$$P = q_i T\bar{C}\,p(N-1)K\,(1 - f_I)(1 - f_m\epsilon_i)(1 - f_m\epsilon_o) \quad (24)$$

For the case of zero initial concentration, we assume firstly that the number of infected passengers is one and thus equation (20) becomes

$$d = \frac{q_i T q_o}{V(\alpha+\beta+\gamma+\delta)}\left(1 - \frac{\left(1-e^{-T(\alpha+\beta+\gamma+\delta)}\right)}{T(\alpha+\beta+\gamma+\delta)}\right) \quad (25)$$

Now let

$$R = \frac{q_i}{q_{i,ref}}\frac{q_o}{q_{o,ref}} \quad (26)$$

where $q_{i,ref}$ and $q_{o,ref}$ are reference values of q_i and q_o for a person at rest, and not speaking. R allows for the effect of exercise and intensity of speaking / singing. The equation for dose becomes

$$d = \frac{q_{i,ref} T q_{o,ref}}{V(\alpha+\beta+\gamma+\delta)}\left(1 - \frac{\left(1-e^{-T(\alpha+\beta+\gamma+\delta)}\right)}{T(\alpha+\beta+\gamma+\delta)}\right) R \quad (27)$$

Values of R, calculated from the data given in Jimenez and Peng are given in table 1. There can be seen to be very large variations in this parameter depending on physical and oral activity.

Equations (23) and (27) give

$$P = \frac{q_{i,ref} T q_{o,ref}}{V(\alpha+\beta+\gamma+\delta)}\left(1 - \frac{\left(1-e^{-T(\alpha+\beta+\gamma+\delta)}\right)}{T(\alpha+\beta+\gamma+\delta)}\right) R\, p(N-1)K(1-f_I)(1-f_m\epsilon_o)(1-f_m\epsilon_i) \quad (28)$$

For long journeys this becomes

$$P_\infty = \frac{q_{i,ref} T q_{o,ref}}{V(\alpha+\beta+\gamma+\delta)}\, R(1-f_m\epsilon_o)(1-f_m\epsilon_i)(N-1)\, pK\,(1-f_I) \quad (29)$$

Values of R		Speaking or singing		
		Not speaking	Speaking quietly	Speaking loudly or singing
Exercise type	At rest	1	5	30
	Light intensity	2.5	12.5	70
	Moderate intensity	14	70	420
	High intensity	70	350	2100

Table 1 Values of the parameter R

Now the simple algebraic formulation of equation (29) allows the interplay between the important parameters to be well appreciated. It shows that infection risk is linearly proportional to exposure time, prevailing infection rate, and inversely proportional to volume of the ventilated space and air exchange rate. It is also proportional to the parameter R, which can be seen to vary very substantially with activity and can increase the infection rate by two or three orders of magnitude. The effect of mask-wearing and population immunity is also clear. Whilst Jimenez and Peng (2021) would acknowledge the approximations made in the model, and also noting that further approximations have been made in deriving equation ((20), the expression seems to be a very useful one to aid in an understanding of the infection problem.

The main issue with this infection model is that it assumes complete mixing of the pathogen throughout the cabin space and does not take account of the elevated concentrations around an infected individual. A possible way to deal with this is set out in Appendix 1. Further work is required in this area.

4. Ventilation of public transport vehicles

4.1 Types of ventilation

Up to this point, the precise nature of vehicle ventilation has not been considered. In this section we look at the different types of ventilation that can occur in different vehicles and how the flow rates through these systems can be determined.

There are three basic types of vehicle ventilation for buses and trains - mechanical ventilation through HVAC systems, ventilation through openings such as windows and doors, and ventilation due to leakage. We consider these in turn below.

4.2 Mechanical ventilation

Mechanical ventilation is through the use of HVAC systems. These are usually commercially designed and supplied, to provide a specific flow rate of air into the vehicle $\dot{m}_{i,HVAC}$. Some systems include the facility for recirculating and cleaning the ingested air, through the use of filters of different types. They tend to have inlets on vehicle roofs as a rule, where the pressures are close to the undisturbed value, but depending on the precise nature of the geometry the flow rates may be to some degree affected by flow induced pressure variations. Some HVAC systems have the facility for a degree of control i.e. varying the flow rate. See Li et al (2019) for a useful overview, albeit in the context of CFD calculations. The air exchange rate from this ventilation mechanism is given by

$$\alpha_{HVAC} = \frac{\sum \dot{m}_{i,HVAC}}{\rho V} \tag{30}$$

$\dot{m}_{i,HVAC}$ for such systems are of the order of 1200 kg/h. giving values a_{HVAC} in a typical train passenger compartment of volume 200m^3 with two HVAC units of 10/h. This is equivalent to a well-ventilated building but somewhat below the 20 to 30/h found in aeroplanes.

4.3 Ventilation through windows and doors

Passenger compartment ventilation through openings is of necessity much more variable than mechanical ventilation. The most common type of ventilation is through windows on the side of vehicles and is obviously a function of vehicle speed. To specify this mode of ventilation, we use the analysis of Straw et al (2000) who defined what they termed the shear layer ventilation due to flow across an opening. Using experimental data from a large cube in the atmospheric boundary layer, they were able to show that the mass flow rate could be approximated by $k\rho Au$ where *k* is a constant (of the order of 0.1), ρ is the density of air, A is the overall opening area, and u is the wind speed across the opening. Applying this to the vehicle case, we write the following expression for ventilation rate due to open windows $\dot{m}_{i,w}$ as

$$\dot{m}_{i,w} = 3600 k \rho v A_{i,w} \tag{31}$$

$A_{i,w}$ is the area of a window opening in m^2 and v is the vehicle speed in m/s. $\dot{m}_{i,w}$ is the mass flow rate in kg/h. The ventilation rate is thus a function of vehicle speed, which matches with experience. The air exchange rate due to windows is thus

$$\alpha_w = \frac{3600\, kv \sum A_{i,w}}{V} \tag{32}$$

This approach is confirmed to some degree by the CFD work of Li et al (2017) who looked at ventilation rates into a school bus. The linear dependence of ventilation flow rates with bus speed was clear, and, although precise opening areas are not given, values of *k* between 0.03 and 0.15 could be calculated making reasonable assumptions. These values varied with the window opening configuration. We will use a value of 0.1 in what follows. Putting in typical values of the parameters for a train carriage of internal volume of 200m^3, a speed of 25m/s and four open windows of 0.05m^2 each gives an air exchange rate a_w of around 9/h which seems reasonable. Increasing the number of open windows to ten gives a high value of a_w of 22.5/h. This high value is consistent with the author's personal (and subjective) experience of travelling on such trains with many windows open. Note however that the air exchange rate can reduce to zero as the speed falls, or if the windows are closed due to low external temperatures.

Some ventilation can also take place through open doors at stations or bus stops. This is difficult to quantify, but in what follows we use expressions analogous to the ones for window ventilation.

$$\dot{m}_{i,d} = 3600k\rho A_{i,d}u \tag{33}$$

$$\alpha_d = \frac{3600ku\sum A_{i,d}}{V} \tag{34}$$

Here $A_{i,d}$ is the area of one door, and u is a nominal wind speed across the door opening, that will be taken as 1m/s in what follows. For the train carriage above, with two door openings of 3m^2 each, this gives a_d as 10.8/h, although as doors will only be open for a small proportion of the time, the average value over a journey will be much less.

4.4 Ventilation by leakage

The third potential source of ventilation is through leakage in the vehicle envelope. This can be conveniently divided into two types. The first, applicable to buses and coaches, is ventilation driven by the relatively large pressure difference between the front and the back of the vehicle, and the second, of more relevance to sealed trains, is due to the pressure difference between the pressure along the sides of the train, and the internal pressure. We consider them in turn.

The first type of leakage can be specified by the orifice type analysis used in building ventilation. The leakage mass flow rate in kg/h is given by the following equation.

$$\dot{m}_l = 3600\rho A_l v C_d \left(\Delta C_p\right)^{0.5} \tag{35}$$

Here A_l is the leakage area, C_d is the discharge coefficient and ΔC_p is the difference in the pressure coefficient between the front and rear of the vehicle. This gives an air exchange rate due to leakage of

$$\alpha_l = \frac{3600A_l v C_d \left(\Delta C_p\right)^{0.5}}{V} \tag{36}$$

For a bus travelling at a speed of 20m/s, with a volume of 100m^3, a discharge coefficient of 0.6, a front to back pressure coefficient difference of 1.0, and a leakage area of 0.01m^2, this gives a value of α_l of 4.3, a not insubstantial value. This is of course very dependent upon vehicle speed.

An analysis of leakage effects along the side of trains is presented in Appendix 2. It is shown there that the leakage through the envelope results in an air exchange rate given by

$$\alpha_l = \frac{3600}{\tau}\frac{\Delta p}{r p_e} \tag{37}$$

Here Δp is the difference between internal and external pressure (usually around 100 Pa); τ is the leakage time constant obtained from full scale tests (around 30 s); p_e is the ambient pressure (10^5 Pa) and r is the ratio of specific heats (=1.4). These figures give the very low value of α_l of 0.1 air changes / hour. Such values are typical, and this type of leakage ventilation will not be considered further in this analysis. See the appendix for further details.

5. Scenario analysis

In this section, we present the results of a simple scenario analysis that investigates the application of the above analysis for different types of vehicle with a range different ventilation systems, running through different transport environments. We consider the following vehicle and ventilation types.

- An air-conditioned diesel train, with controllable HVAC systems.
- A window and door ventilated diesel train.
- A bus ventilated by windows, doors, and externally pressure generated leakage.

Two journey environments are considered.

- For the trains, a one-hour commuter journey as shown in figure 1, beginning in an inner-city enclosed station, running through an urban area with two stations and two tunnels, and then through a rural area with three stations (figure 1).
- For buses, a one-hour commuter journey, with regular stops, through city centre, suburban and rural environments (figure 2).

Results are presented for the following scenarios.

- Scenario 1. Air-conditioned train on the rail route, with HVACs operating at full capacity throughout.
- Scenario 2. As scenario 1, but with the HVACs turned to low flow rates in tunnels and enclosed stations, where there are high levels of pollutants.
- Scenario 3. Window ventilated train on rail route with windows open throughout and doors opened at stations.
- Scenario 4. As scenario 3, but with windows closed.
- Scenario 5. Window, door and leakage ventilated bus on bus route with windows open throughout and doors opened at bus stops.
- Scenario 6. As scenario 5, but with windows closed.

Details of the different environments and scenarios are given in tables 2 and 3. Realistic, if somewhat arbitrary levels of environmental and exhaust pollutants are specified for the different environments - high concentrations in cities and enclosed railway and bus stations and lower concentrations in rural areas. The air exchange rates from different mechanisms are also specified, with the values given from the analysis of section 4, specifically using equation (32) for window ventilation, equation (34) for door ventilation an equation (36) for leakage ventilation. Note that, in any development of this methodology, more detailed models of the exhaust emissions could be used that relate concentrations at the HVAC systems and window openings to concentrations at the stack, which would allow more complex speed profiles to be investigated, with acceleration and deceleration phases.

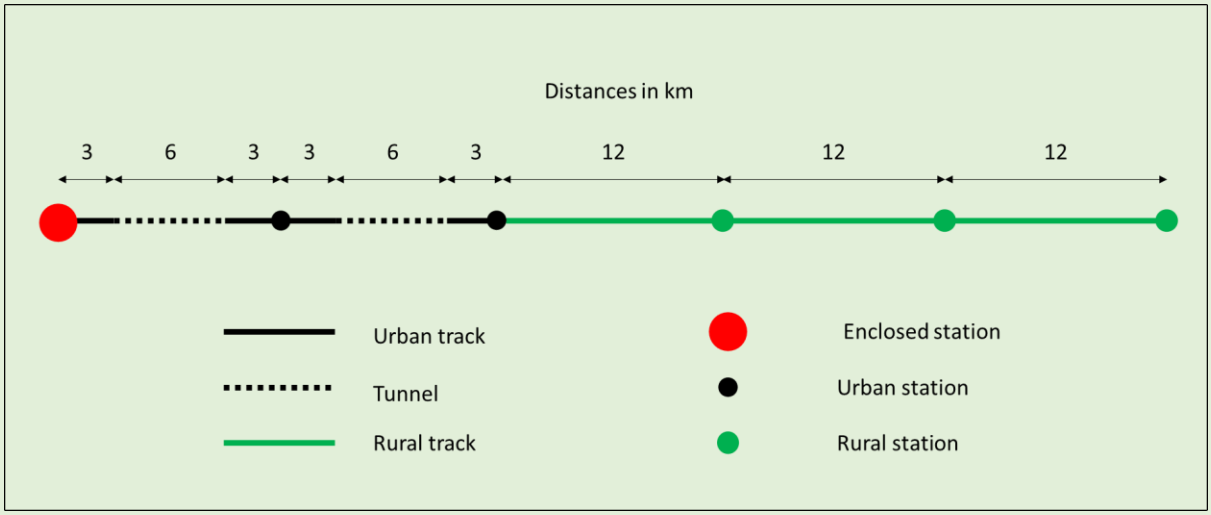

Figure 1. The rail route

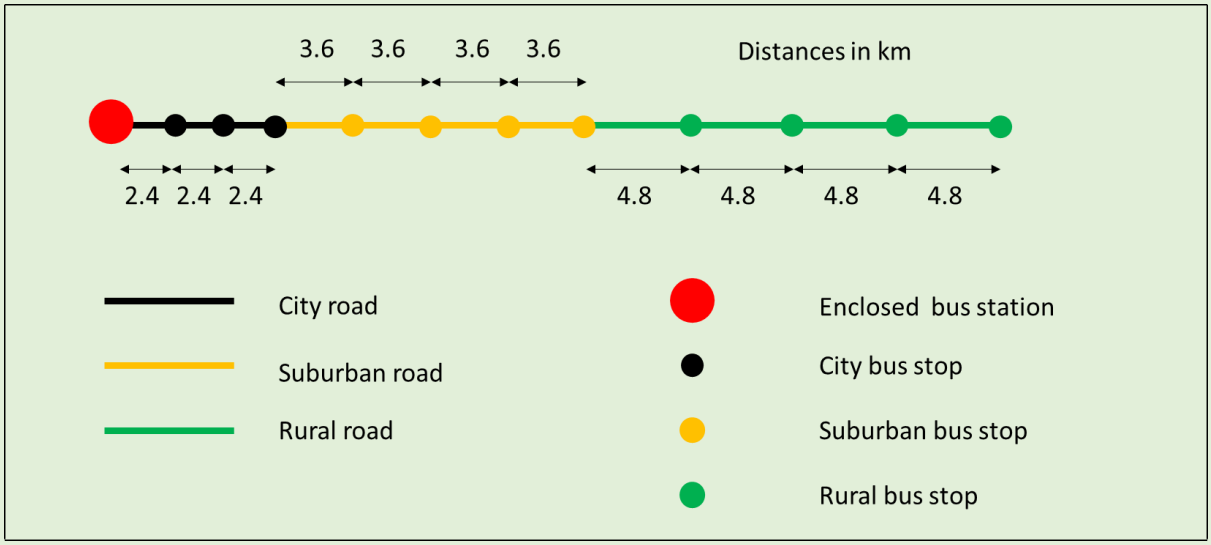

Figure 2. The bus route

	Time (min)	Concentrations						Air exchange rates / h					
		NO_2 (μg/m^3)		PM10 (μg/m^3)		CO_2 (ppm)		Scenario 1	Scenario 2	Scenario 3		Scenario 4	
		Environment	Exhaust	Environment	Exhaust	Environment	Exhaust	Full HVAC	Controlled HVAC	Window	Door	Window	Door
Enclosed station	0-10	300	0	50	0	600	0	10	1	0	10.8	0	10.8
Urban track	10-12	100	200	30	100	300	500	10	10	9	0	0	0
Tunnel	12-16	100	200	100	100	300	500	10	1	9	0	0	0
Urban track	16-18	100	200	30	100	300	500	10	10	9	0	0	0
Urban station	18-20	100	0	30	0	300	0	10	10	0	10.8	0	10.8
Urban track	20-22	100	200	30	100	300	500	10	10	9	0	0	0
Tunnel	22-26	100	200	100	100	300	500	10	1	9	0	0	0
Urban track	26-28	100	200	30	100	300	500	10	10	9	0	0	0
Urban station	28-30	100	0	30	0	300	0	10	10	0	10.8	0	10.8
Rural track	30-38	50	200	20	100	300	500	10	10	9	0	0	0
Rural station	38-40	50	0	20	0	300	0	10	10	0	10.8	0	10.8
Rural track	40-48	50	200	20	100	300	500	10	10	9	0	0	0
Rural station	48-50	50	0	20	0	300	0	10	10	0	10.8	0	10.8
Rural track	50-58	50	200	20	100	300	500	10	10	9	0	0	0
Rural station	58-60	50	0	20	0	300	0	10	10	0	10.8	0	10.8

Operating speed on open track and in tunnel 25m/s; Cabin volume 200; Number of passengers 60; Number of infected passengers 1; Carbon Dioxide emitted per passenger 0.0216m^3/h; Pathogen quanta emitted per infected passenger 10; Recirculation air exchange rate (Scenarios 1 and 2) 3/h; window opening area (Scenario 3) 0.2m^2; door opening area (Scenario 4) 6m^2; particulate and pathogen deposition rate 3.3/h; pathogen decay rate 1.6/h.

Table 2. The rail journey parameters

	Time (min)	Concentrations			Air exchange rates / h					
		NO_2	PM10	CO_2	Scenario 5			Scenario 6		
		Environment	Environment	Environment	Window	Door	Leakage	Window	Door	Leakage
Bus station	0-5	300	50	600	0	10.8	0	0	10.8	0
City road	5-9	200	40	500	7.2	0	2.16	0	0	2.16
City bus stop	9-10	200	40	500	0	10.8	0	0	10.8	0
City road	10-14	200	40	500	7.2	0	2.16	0	0	2.16
City bus stop	14-15	200	40	500	0	10.8	0	0	10.8	0
City road	15-19	200	40	500	7.2	0	2.16	0	0	2.16
City bus stop	19-20	200	40	500	0	10.8	0	0	10.8	0
Suburban road	20-24	100	30	300	10.8	0	3.24	0	0	3.24
Suburban bus stop	24-25	100	30	300	0	10.8	0	0	10.8	0
Suburban road	25-29	100	30	300	10.8	0	3.24	0	0	3.24
Suburban bus stop	29-30	100	30	300	0	10.8	0	0	10.8	0
Suburban road	30-34	100	30	300	10.8	0	3.24	0	0	3.24
Suburban bus stop	34-35	100	30	300	0	10.8	0	0	10.8	0
Suburban road	35-39	100	30	300	10.8	0	3.24	0	0	3.24
Suburban bus stop	39-40	100	30	300	0	10.8	0	0	10.8	0
Rural road	40-44	50	20	300	14.4	0	4.32	0	0	4.32
Rural bus stop	44-45	50	20	300	0	10.8	0	0	10.8	0
Rural road	45-49	50	20	300	14.4	0	4.32	0	0	4.32
Rural bus stop	49-50	50	20	300	0	10.8	0	0	10.8	0
Rural road	50-54	50	20	300	14.4	0	4.32	0	0	4.32
Rural bus stop	54-55	50	20	300	0	10.8	0	0	10.8	0
Rural road	55-59	50	20	300	14.4	0	4.32	0	0	4.32
Rural bus stop	59-60	50	20	300	0	10.8	0	0	10.8	0

Operating speed on rural roads, suburban roads and city roads 20m/s, 15m/s and 10m/s respectively; Cabin volume 100 m^3; Number of passengers 30; Number of infected passengers 1; Carbon Dioxide emitted per passenger 0.0216m^3/h; Pathogen quanta emitted per infected passenger 10; Recirculation air exchange rate (Scenarios 1 and 2) 3/h; window opening area (Scenario 5) 0.2m^2; door opening area (Scenario 4) 3m^2; leakage area 0.1m^2; particulate and pathogen deposition rate 3.3/h; pathogen decay rate 1.6/h.

Table 3. Bus journey parameters

The results of the analysis are shown in figures 3 and 4 below for the train and bus scenarios respectively. Both figures show time histories of concentrations for NO2, PM2.5, CO2 and Covid-19, together with the external concentrations of the pollutants.

For Scenario 1, with constant air conditioning, all species tend to an equilibrium value that is the external value in the case of NO2 and PM2.5, slightly higher than the external value for CO2 due to the internal generation and a value fixed by the emission rate for Covid 19.

For Scenario 2, with low levels of ventilation in the enclosed station and in the tunnels, NO2 and PM2.5 values are lower than scenario 1 at the start of the journey where the lower ventilation rates are used, but CO2 and Covd-19 concentrations are considerably elevated. When the ventilation rates are increased in the second half of the journey all concentrations approach those of Scenario 1.

The concentration values for scenario 3, with open windows, match those of Scenario 1 quite closely as the specified ventilation rates are similar. However, for Scenario 4, with windows shut and only door ventilation at stations, such as might be the case in inclement weather, the situation is very different, with steadily falling levels of NO2 and PM2.5, but significantly higher values of CO2 and Covid-19. The latter clearly show the effect of door openings at stations.

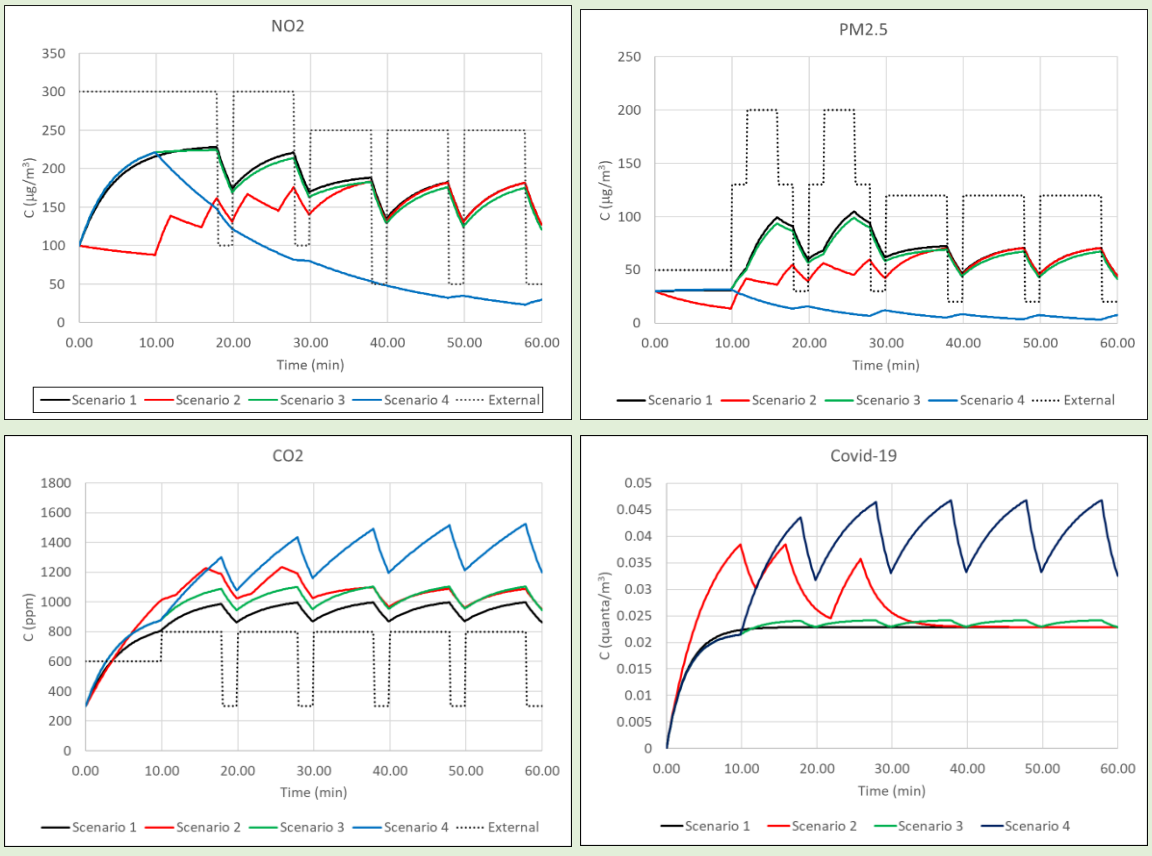

Figure 3. Train scenarios 1 to 4

Now consider the bus scenarios in figure 4. For both Scenario 5 with open windows and doors, and Scenario 6 with closed windows and open doors, the NO2 and PM2.5 values tend towards the ambient concentrations and thus fall throughout the journey as the air becomes cleaner in rural areas. The internally generated CO2 and Covid-19 concentrations for CO2 and Covid-19 are however very much higher for Scenario 6 than for Scenario 5.

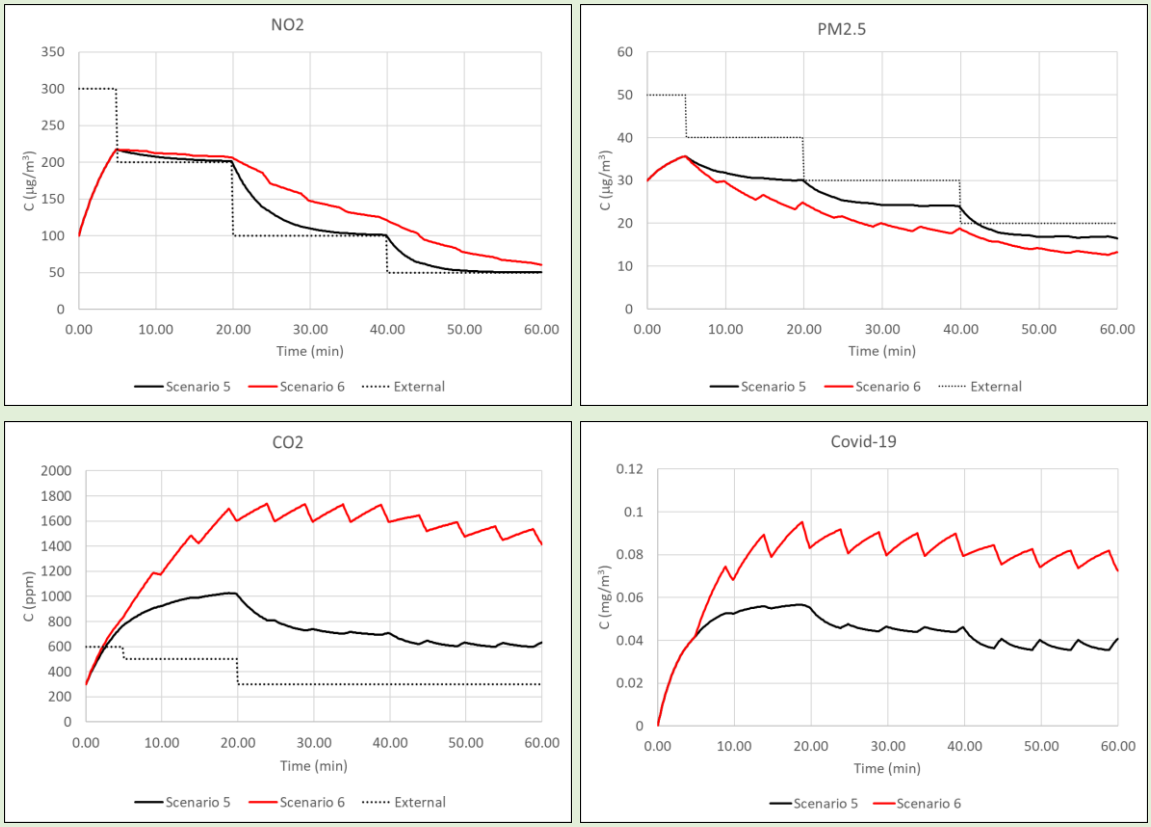

Figure 4. Bus scenarios 5 and 6

The average values of concentration for all the scenarios is given in Table 4. The dose and, for Covid-19, the infection probability, are proportional to these concentrations. For NO2 and PM10 the average concentrations reflect the average external concentrations, and, with the exception of Scenario 4, where there is low air exchange with the external environment for part of the journey. The average concentrations for CO2 and Covid-19 for the less ventilated Scenarios 4 and 6 are significantly higher than the other. For Covid-19, the effect of closing windows on window ventilated trains and buses raises the concentrations, and thus the infection probabilities, by 60% and 76% respectively.

	NO2 (μg/m^3)	PM2.5 (μg/m^3)	CO2 (ppm)	Covid-19 (quanta/m^3)
Scenario 1	183	63	890	0.022
Scenario 2	145	49	1015	0.026
Scenario 3	179	60	978	0.022
Scenario 4	96	13	1193	0.036
Scenario 5	125	25	745	0.043
Scenario 6	146	21	1452	0.076

Table 4. Average concentrations

6. Closing comments

The major strength of the methodology described above is its ability, in a simple and straightforward way, to model pollutant and pathogen concentrations for complete journeys, and to investigate the efficacy of various operational and design changes on these concentrations. It could thus be used, for example, to develop HVAC operational strategies for a range of different journey types. That being said, there is much more that needs to be done - for example linking the methodology with calculations of exhaust dispersion around vehicles, with models of particulate resuspension or with models of wind speed and direction variability. It has also been pointed out above that the main limitation of the infection model is the assumption of complete mixing, and a possible way forward has been proposed that might overcome this. Nonetheless the model has the potential to be of some utility to public transport operators in their consideration of pollutant and pathogen concentrations and dispersion within their vehicles.

References

Anderson, M. H. G., Johannesson, S., Fonseca, A. S., Clausen, P. A., Saber, A. T., Roursgaard, M., Loeschner, K., Koponen, I. K., Loft, S. and VogeL, U. 2019. Exposure to air pollution inside electric and diesel-powered passenger trains. Environmental science and technology, 53, 4579-4587. https://doi.org/10.1021/acs.est.8b06980

Andersen, M.H.G., Frederiksen, M., Saber, A.T., Wils, R.S., Fonseca, A.S., Koponen, I.K., Johannesson, S., Roursgaard, M., Loft, S., Møller, P., Vogel, U., 2019. Health effects of exposure to diesel exhaust in diesel-powered trains. Part. Fibre Toxicol. 16, 1–14. https://doi.org/10.1186/s12989-019-0306-4

J. T. G Batutay, Cabanban, H. S. Serate, F P. S. Quito J. D. and Umali R. D. 2020 Quantitative and Qualitative Analysis of Indoor Air Quality inside the MRT 3 Train Cabins, Proceedings of the 5th NA International Conference on Industrial Engineering and Operations Management, Detroit, Michigan, USA, http://www.ieomsociety.org/detroit2020/papers/29.pdf

Braniš M, m. 2006. the contribution of ambient sources to particulate pollution in spaces and trains of the Prague underground transport system. Atmospheric Environment, 40, 348-356. https://doi.org/10.1016/j.atmosenv.2005.09.060

Buitrago, N., Savdie, J., Almeida, S. and Verde, S. C. 2021. Factors affecting the exposure to physicochemical and microbiological pollutants in vehicle cabins while commuting in Lisbon. Environmental Pollution, 270, 116062. https://doi.org/10.1016/j.envpol.2020.116062

CDC, 2021 https://www.cdc.gov/niosh/idlh/124389.html

Cha, Y., Abbasi, S. and Olofsson, U. 2018a. Indoor and outdoor measurement of airborne particulates on a commuter train running partly in tunnels. Proceedings of the Institution of Mechanical Engineers, Part F: Journal of Rail and Rapid Transit, 232, 3-13. https://doi.org/10.1177/0954409716642492

Cha, Y., Tu, M., Elmgren, M., Silvergren, S. andOlofsson, U. 2018b. Factors affecting the exposure of passengers, service staff and train drivers inside trains to airborne particles. Environmental research, 166, 16-24. https://doi.org/10.1016/j.envres.2018.05.026

Chaudhry S K, Elumalai S P, 2020, The influence of school bus ventilation scenarios over in-cabin PM number concentration and air exchange rates, Atmospheric Pollution Research, 11, 8, 1396-1407, ISSN 1309-1042, https://doi.org/10.1016/j.apr.2020.05.021

Cheng, Y.-H., Liu, Z.-S. and Yan, J.-W. 2012. Comparisons of PM10, PM2. 5, particle number, and CO2 levels inside metro trains between traveling in underground tunnels and on elevated tracks. Aerosol and Air Quality Research, 12, 879-891. https://doi.org/10.4209/aaqr.2012.05.0127

Comunian S, Dario Dongo D, Milani C, Paola Palestini P, 2020, Air Pollution and COVID-19: The Role of Particulate Matter in the Spread and Increase of COVID-19's Morbidity and Mortality, International Journal of Environmental Research for Public Health, 17, 12, 4487, https://doi.org/10.3390/ijerph17124487

EU, 2021 https://ec.europa.eu/environment/air/quality/standards.htm

Font A, Tremper A, Lin C, Priestman M, Marsh D, Woods M, Heal M, Green D, 2020, Air quality in enclosed railway stations: Quantifying the impact of diesel trains through deployment of multi-site measurement and random forest modelling, Environmental Pollution, 262, 114284, ISSN 0269-7491, https://doi.org/10.1016/j.envpol.2020.114284

Hickman A, Baker C, Cai X, Delgado-Saborit J, Thornes J, 2018, Air Quality Evaluation at Birmingham New Street Railway Station, Proceedings of the Institution of Mechanical Engineers, Part F: Journal of Rail and Rapid Transit, http://dx.doi.org/10.1177/0954409717752180

Hicks W, Beevers S, Tremper A, Stewart G, Priestman M, Kelly F, Lanoisellé M, Lowry D, Green Det al., 2021, Quantification of non-exhaust particulate matter traffic emissions and the impact of COVID-19 lockdown at London Marylebone Road, Atmosphere, 12, 1-19, ISSN: 2073-4433, https://doi.org/10.3390/atmos12020190

Jeong, C.-H., Traub, A. and Evans, G. J. 2017. Exposure to ultrafine particles and black carbon in diesel-powered commuter trains. Atmospheric Environment, 155, 46-52. https://doi.org/10.1016/j.atmosenv.2017.02.015

Jimenez J, Peng Z 2021, COVID-19 Aerosol Transmission Estimator, https://tinyurl.com/covid-estimator

Li F, Lee E S, Zhou B, Liu J, Zhu Y, 2017, Effects of the window openings on the micro-environmental condition in a school bus, Atmospheric Environment, 167, 434-443, ISSN 1352-2310, https://doi.org/10.1016/j.atmosenv.2017.08.053

Li X, Wu F, Tao Y, Yang M, Newman R, Vainchtein D, 2019 Numerical study of the air flow through an air-conditioning unit on high-speed trains, Journal of Wind Engineering and Industrial Aerodynamics, 187, 26-35, https://doi.org/10.1016/j.jweia.2019.01.015

Maggos, T., Saraga, D., BairachtarI, K., Tzagkaroulaki, I., Pateraki, S., Vasilakos, C., Makarounis, C., Stavdaris, A., Danias, G. & Anagnostopoulos, G. 2016. Air quality assessment in passenger trains: the impact of smokestack emissions. Air Quality, Atmosphere and Health, 9, 391-401. https://doi.org/10.1007/s11869-015-0348-1

Mein S A, Annesi-Maesano I, Rice M B, 2020, COVID-19 Pandemic: A Wake-Up Call for Clean Air, Annals of the American Thoracic Society, 18, 9 https://doi.org/10.1513/AnnalsATS.202012-1542VP PubMed: 33821776

Miller S L, Nazaroff W W, Jimenez J L, Boerstra A, Buonanno G, Dancer S J, Kurnitski J, Marr L C, Morawska L, Noakes C, 2021, Transmission of SARS-CoV-2 by inhalation of respiratory aerosol in the Skagit Valley Chorale superspreading event, Indoor Air, 31, 314–323, https://doi.org/10.1111/ina.12751

Nor, N.S.M., Yip, C.W., Ibrahim, N. et al, 2021, Particulate matter (PM2.5) as a potential SARS-CoV-2 carrier. Science Report 11, 2508 https://doi.org/10.1038/s41598-021-81935-9

Park, D.-U. and Ha, K.-C. 2008. Characteristics of PM10, PM2. 5, CO2 and CO monitored in interiors and platforms of subway train in Seoul, Korea. Environment International, 34, 629-634. https://doi.org/10.1016/j.envint.2007.12.007

Peng S, Chen Q, Liu E, 2020 The role of computational fluid dynamics tools on investigation of pathogen transmission: Prevention and control, Science of The Total Environment, 746, 142090, ISSN 0048-9697, https://doi.org/10.1016/j.scitotenv.2020.142090

Travaglio M, Yu Y, Popovic R, Selley L, Leal N S, Martins L M, 2021, Links between air pollution and COVID-19 in England, Environmental Pollution, 268, A, 115859, ISSN 0269-7491, https://doi.org/10.1016/j.envpol.2020.115859

Straw M, Baker C, Robertson A 2000, Experimental measurements and computations of the wind induced ventilation of a cubic structure, Journal of Wind Engineering and Industrial Aerodynamics 88, 213-230, http://dx.doi.org/10.1016/S0167-6105(00)00050-7

Wang C, Prathe K, Sznitman, Jimenez J, Lakdawala S, Tufekci Z, Marr L, 2021, Airborne transmission of respiratory viruses, Science, 373, 6558, https://doi.org/10.1126/science.abd9149

Wang H, Lin M, Chen Y, 2014, Performance evaluation of air distribution systems in three different China railway high-speed train cabins using numerical simulation, Building Simulation, 7, 6, 629-638, https://doi.org/10.1007/s12273-014-0168-5

Zhang, L. and Li, Y. 2012. Dispersion of coughed droplets in a fully occupied high-speed rail cabin. Building and Environment, 47, 58-66. https://doi.org/10.1016/j.buildenv.2011.03.015

Appendix 1. A possible method for allowing for non-spatially uniform passenger cabin concentrations

The analytical method in the main text gives the approximate probability of an infection occurring amongst *N* passengers, where one is infected, assumed complete mixing of the pathogen in the cabin (equation (24)). In this short appendix we propose a way in which spatially uneven concentrations of pathogen could be allowed for.

If we assume that there are just two passengers where one is infected, we obtain from equation (24) the following for the probability of a passenger in seat *i* being infected by a passenger in seat *j*.

$$P_{i,j} = q_i T \bar{C}_{i,j}\, p\, K\, (1 - f_I)(1 - f_m \epsilon_i)(1 - f_m \epsilon_o)$$

Here $\bar{C}_{i,j}$ is the time average concentration of pathogen in seat *i* due to an infected passenger in seat *j*. The total infection probability for *N* passengers is obtained by finding the average probability for all possible non-infected passenger and infected passenger positions (*s*) and multiplying by $(N-1)$.

$$P = (N-1)\frac{(\sum_{i=1 to\ s, j=1\ to\ s} P_{i,j})}{s^2}$$

This gives

$$P = q_i T\, \frac{(\sum_{i=1 to\ s, j=1\ to\ s} \bar{C}_{i,j})}{s^2} p(N-1) K\, (1 - f_I)(1 - f_m \epsilon_i)(1 - f_m \epsilon_o)$$

We define a factor *F*

$$F = \frac{\sum_{i=1 to\ s, j=1\ to\ s} \bar{C}_{i,j}}{s^2 \bar{C}}$$

The overall infection probability thus becomes

$$P = q_i T\, F\, \bar{C}\, p(N-1) K\, (1 - f_I)(1 - f_m \epsilon_i)(1 - f_m \epsilon_o)$$

This is of course identical to equation (24) with the addition of the parameter F. In principle, this parameter could be found by a CFD calculation of the internal flow in a specific vehicle and tracking the concentration of (say) carbon dioxide from each person throughout the cabin to find the resulting concentration at every other passenger position, to give the function $\bar{C}_{i,j}$ and thus F. $\bar{C}_{i,j}$ can be expected to be well above unity when the seats *i* and *j* are close, and well below unity for all other cases. Whether or not it will be above or below 1.0 will depend upon the vehicle, the seating arrangement etc. Thus, a CFD calculation of the internal flow within a vehicle could be used to calibrate the simple model outlined here for predicting infection risk during specific journeys, with specific ventilation strategies and searing arrangements.

Appendix 2. Leakage through the vehicle envelope

The leakage into a train cabin can be modelled in one of two ways - either as a large number of small pipes, or as a number of orifices. The basics of the two methods are shown in table A2 below. They begin in row 1 with the conservation of mass where the leakage mass flow rate is equal to the rate of change of internal mass and specified by either the pipe flow energy loss equation of the orifice discharge equation. Here ρ is the external air density, A is the total leakage area, w is the leakage velocity, V is the cabin volume, ρ_i is the internal density, d_1 is the leakage pipe diameter, l_1 is the leakage pipe length, f is the Darcy friction factor, C is the orifice coefficient and Δp is the difference between the internal and external pressure $(p_i - p_e)$. Assumptions are then made for the Darcy friction factor and orifice coefficient (row 2). Both are given in their low Reynolds number form. Here k_1 and k_2 are constants, μ is the dynamic viscosity of air and d_2 is the leakage orifice diameter. The adiabatic gas law is then used to relate the rate of change of internal pressure to that of internal density (row 3). Here r is the ratio of specific heats. The equations in rows 1 to 3 are then use to derive a relationship between the leakage velocity and the pressure difference (row 4) and between the rate of change of internal pressure and the pressure difference (row 5). Leakage time constants are then defined in row 6, and these are then used to rewrite the leakage velocity and pressure rate of change equations in much simpler form in rows 7 and 8. Written in this form the two methods are actually equivalent. The pressure rate of change equation in row 8 is the form used in calculating train leakage from pressure decay in full scale tests, where the internal pressure is raised to a high value and then allowed to decay. In these experiments the time constant τ is measured. For sealed trains this parameter has values of around 20 to 60 seconds. Finally in row 9 the expression for air exchange rate is given, which is again identical for both methods. Substituting typical values for τ = 30 s (=0.0083 h); Δp = 100 Pa; p_e = 10^5 Pa and γ =1.4 gives a value of air changes per hour of less than 0.1. Higher values of Δp are possible when trains experience pressure transients passing through tunnels (perhaps as high as 2000 Pa, but these will be very transitory and the briefly increased air exchange rates will not greatly contribute to cabin ventilation. The use of such formulae in the calculation of internal pressures as trains pass through tunnels is however important when passenger aural comfort is being considered.

	Pipe model	Orifice model
1. Conservation of mass for internal flow	$\rho A w = V\frac{d\rho_i}{dt} = -A\left(\frac{d_1}{f l_1}\right)^{0.5}(2\rho\Delta p)^{0.5}$	$\rho A w = V\frac{d\rho_i}{dt} = -AC(2\rho\Delta p)^{0.5}$
2. Friction factors	$f = \frac{k_1\mu}{\rho w d_1}$	$C = k_2\left(\frac{\rho w d_2}{\mu}\right)^{0.5}$
3. Adiabatic gas law	$\frac{dp_i}{dt} = rp_e\frac{d\rho_i}{dt}$	
4. Leakage velocity and pressure difference	$w = \frac{2{d_1}^2}{l_1 k_1 \mu}\Delta p$	$w = \frac{2 d_2 {k_2}^2}{\mu}\Delta p$
5. Leakage pressure rate of change and pressure difference	$\frac{dp_i}{dt} = -\frac{2A{d_1}^2 rp_e}{l_1 k_1 \mu V}\Delta p$	$\frac{dp_i}{dt} = -\frac{2A d_2 {k_2}^2 rp_e}{\mu V}\Delta p$
6. Leakage time constant	$\tau = \frac{l_1 k_1 \mu V}{2A{d_1}^2 rp_e}$	$\tau = \frac{\mu V}{2A d_2 {k_2}^2 rp_e}$
7. Leakage velocity and pressure difference	$w = \frac{V}{A rp_e}\frac{\Delta p}{\tau}$	
8. Leakage pressure rate of change and pressure difference	$\frac{dp_i}{dt} = -\frac{\Delta p}{\tau}$	
9. Air changes per hour	$a = \frac{1}{\tau}\frac{\Delta p}{rp_e} = \frac{Aw}{V}$	

Table A2. Leakage calculations